Four Mutant Alleles Elucidate the Role of the G2 Protein in the Development of C_4 and C_3 Photosynthesizing Maize Tissues

Lizzie Cribb,[1] Lisa N. Hall[2] and Jane A. Langdale

Department of Plant Sciences, University of Oxford, Oxford OX1 3RB, United Kingdom

Manuscript received February 22, 2001
Accepted for publication July 9, 2001

ABSTRACT

Maize leaf blades differentiate dimorphic photosynthetic cell types, the bundle sheath and mesophyll, between which the reactions of C_4 photosynthesis are partitioned. Leaf-like organs of maize such as husk leaves, however, develop a C_3 pattern of differentiation whereby ribulose bisphosphate carboxylase (RuBPCase) accumulates in all photosynthetic cell types. The *Golden2* (*G2*) gene has previously been shown to play a role in bundle sheath cell differentiation in C_4 leaf blades and to play a less well-defined role in C_3 maize tissues. To further analyze *G2* gene function in maize, four *g2* mutations have been characterized. Three of these mutations were induced by the transposable element *Spm*. In *g2-bsd1-m1* and *g2-bsd1-s1*, the element is inserted in the second intron and in *g2-pg14* the element is inserted in the promoter. In the fourth case, *g2-R*, four amino acid changes and premature polyadenylation of the *G2* transcript are observed. The phenotypes conditioned by these four mutations demonstrate that the primary role of G2 in C_4 leaf blades is to promote bundle sheath cell chloroplast development. C_4 photosynthetic enzymes can accumulate in both bundle sheath and mesophyll cells in the absence of G2. In C_3 tissue, however, G2 influences both chloroplast differentiation and photosynthetic enzyme accumulation patterns. On the basis of the phenotypic data obtained, a model that postulates how G2 acts to facilitate C_4 and C_3 patterns of tissue development is proposed.

AT maturity, the C_4 plant maize exhibits both C_4 and C_3 photosynthesizing tissues and thus different developmental strategies must be adopted in a tissue-specific manner. In C_4 tissues such as mature leaf blades, distinct bundle sheath and mesophyll cells surround the vasculature such that veins are separated by a maximum of four photosynthetic cells (two bundle sheath and two mesophyll). Bundle sheath and mesophyll cells each develop plastids with a characteristic ultrastructure and accumulate a specific complement of photosynthetic enzymes (reviewed in Edwards and Walker 1983; Nelson and Langdale 1992; Hall and Langdale 1996). In the bundle sheath cells, chloroplasts are agranal and accumulate the photosynthetic enzymes ribulose bisphosphate carboxylase (RuBPCase) and NADP-dependent malic enzyme (ME). In the mesophyll cells, chloroplasts contain stacked grana and accumulate pyruvate phosphate dikinase (PPdK) and NADP-dependent malate dehydrogenase (MDH). Phosphoenolpyruvate carboxylase (PEPCase) accumulates in the cytoplasm of C_4 mesophyll cells and acts as the primary carboxylating enzyme. An alternative differentiation pattern is observed in C_3 tissue such as husk leaves, where veins are separated by more than four cells. Bundle sheath cells surrounding the veins and the mesophyll cells that are directly adjacent to them develop C_4 characteristics as above. However, mesophyll cells at a greater distance from a vein (referred to here as C_3 mesophyll cells) develop chloroplasts with stacked grana in which RuBPCase acts as the primary carboxylating enzyme. A third differentiation pattern is seen in etiolated leaf blade tissue where bundle sheath and mesophyll cells develop identical etioplasts in which RuBPCase accumulates but is not functional. Transcripts encoding the cell-specific C_4 photosynthesizing enzymes also accumulate in etiolated tissue but the corresponding proteins are not present. Therefore, in terms of enzyme accumulation, etiolated tissue represents a C_3 but nonphotosynthesizing state.

The differentiation patterns described above demonstrate that light and cell position relative to a vein are important factors in determining whether cells adopt a C_4 bundle sheath, C_4 mesophyll, or C_3 mesophyll fate (Langdale *et al.* 1988b; Langdale and Nelson 1991). However, it was characterization of the *g2-bsd1-m1* (*golden2-bundle sheath defective1-mutable1*) mutant that provided the first insight into a specific gene that regulates photosynthetic differentiation patterns in maize (Langdale and Kidner 1994). The *G2* gene encodes a novel transcriptional activator (Hall *et al.* 1998; Rossini *et al.* 2001). In *g2-bsd1-m1* mutant leaf blades, both chloroplast development and the accumulation of pho-

Corresponding author: Jane A. Langdale, Department of Plant Sciences, University of Oxford, South Parks Rd., Oxford OX1 3RB, United Kingdom. E-mail: jane.langdale@plants.ox.ac.uk

[1]*Present address:* Genome Biology, Current Science Group, Middlesex House, London W1P 6LB, United Kingdom.

[2]*Present address:* Syngenta, Jealott's Hill Research Station, Bracknell, Berks RG12 6EY, United Kingdom.

tosynthetic enzymes were found to be aberrant in bundle sheath cells yet mesophyll cells developed appropriately (Langdale and Kidner 1994). Thus, G2 was proposed to specifically regulate photosynthetic development of bundle sheath cells in C_4 tissue. In C_3 tissue, however, the mutant phenotype suggested a non-cell-specific role for G2. In etiolated leaves of mutant plants, RuBPCase was not present in either bundle sheath or mesophyll cells despite the fact that etioplast development was perturbed only in bundle sheath cells (Langdale and Kidner 1994). In leaf sheath tissue, a non-cell-specific role for G2 was also inferred as mutant leaf sheaths are completely white.

The complexity of the *g2-bsd1-m1* mutant phenotype has previously obscured our understanding of *G2* gene function. In an attempt to reduce this complexity, we have now characterized an allelic series of *g2* mutations after introgression into the maize inbred line B73. Because introgression suppressed the phenotypic severity of some aspects of the mutant phenotype, the primary effects of the mutation were revealed.

MATERIALS AND METHODS

Plant material: The maize inbred line used throughout this study, B73, was a gift from Pioneer HiBred. The *g2-bsd1-m1* and *g2-bsd1-s1* maize lines were described previously (Langdale and Kidner 1994; Hall *et al.* 1998). *g2-pg14* and *g2-R* stocks were obtained from the Maize Genetics Stock Centre. Near-isogenic stocks segregating each allele were obtained by backcrossing four times into the B73 inbred line. Mutant individuals were harvested from these families.

Growth conditions: Seedlings were germinated and grown in a growth chamber maintained at 25° with a 16-hr moderate light (100 $\mu E\ m^{-2}\,sec^{-1}$)/8-hr dark cycle. Plastochron 1 to 5 (P1-5) leaf primordia were harvested 3 days after planting when seedlings were 1.5–2 cm tall and all the seedling leaves were still enclosed within the coleoptile. Whole shoots were excised from the plants 3–4 mm above the mesocotyl, the coleoptile was removed, and each sample was stored individually. Seedlings were then returned to the growth chamber until mutant plants could be identified. Third leaves from light-grown seedlings were harvested 15–20 days after planting, as the fourth leaf was emerging. At this stage, the middle of the third leaf blade was expanded but cells at both the base and the tip were still developing. The leaf sheaths were harvested intact and leaf blades were divided into base and tip sections.

Etiolated plants were germinated and grown in vermiculite in complete darkness at 25° for 7 days and harvested under green safelight. Light-shifted (greening) seedlings were germinated and grown in complete darkness for 6 days and then moved to a growth chamber for one 24-hr light/dark cycle, as described above, before harvesting.

Preparation of DNA: Genomic DNA was isolated from leaf tissue according to Chen and Dellaporta (1994).

Amplification of DNA fragments by the polymerase chain reaction: The polymerase chain reaction (PCR) was used to generate fragments containing junctions of *Spm* and *G2* sequence from *g2-bsd1-m1, g2-bsd1-s1,* and *g2-pg14* alleles. The following primer combinations were used: tor7 (5′-GGACGC CGGAGCTGCA-3′) and R3 (5′-TCGGCTTATTTCAGTAA GAGTGTG-3′) to amplify the 5′ function fragment in *g2-bsd1-m1*; tor6 (5′-GCCTCCGCCTCCCGCGC-3′) and L1 (5′-ACGC CGCTGGCTAGACTGGAGAGA-3′) to amplify the 3′ junction fragment in *g2-bsd1-m1* and *g2-bsd1-s1*; 1-9 (5′-GACCCGGCTA GAGCTATAAAGC-3′) and L1 to amplify the 5′ junction fragment from *g2-pg14*; and 30-4 (5′-GTCCAGGAGGTTGTC GTCC-3′) and R3 to amplify the 3′ junction fragment in *g2-pg14*.

PCR was also used to generate genomic DNA fragments corresponding to each exon of G2. The primers were designed to the G2 sequence and the following combinations were used: 1-9 (as above) and 5-5 (5′-GTACCTTCACCTTGCGCTTGC CGC-3′) to amplify exon 1; tor7 (as above) and 2-5 (5′-GTA CCTGGAGGTGGCTGGCAATGTTGT-3′) to amplify exon 2; 2-3 (5′-AGAAGTACCGGTCGCACAGAAAGC-3′) and 2-4 (5′-GCTGTACTGCTGGTGCCAGAACGC-3′) to amplify exon 3; 2-1 (5′-GCTGCCAGGAAATGGGGCCCACAG-3′) and 2-2 (5′-GTGCGCTTGGAGCTCCAGATGCAG-3′) to amplify exon 4; 48-9 (5′-GTCCAAGGAGAGCATCGACGCAGC-3′) and 10-2 (5′-GCATGTAGCTAGCTAGCAGCTCAC-3′) to amplify exon 5. The PCR-amplified products were cloned into pGEM T-Easy vector (Promega, Madison, WI) and sequenced.

Amplification of cDNA fragments by RT-PCR: Reverse transcriptase PCR (RT-PCR) was used to generate cDNA fragments spanning exons 1–4 of G2. The primers were designed to the G2 sequence and the following combinations were used: 1-1 (5′-GCTCAGCTCACTCTTCATTAAGCG-3′) and tor6 (as above) to amplify exons 1–3 and 2-3 (as above) and 2-2 (as above) to amplify exons 3–4. The PCR-amplified products were cloned into pGEM T-Easy vector (Promega) and sequenced.

Identification of polyadenylation sites by 3′-RACE: To identify the sites of polyadenylatin in the *g2R* allele, 3′ rapid amplification of cDNA ends (RACE) was used. Reactions were performed using a 3′-RACE kit (Boehringer Mannheim, Indianapolis) using 48-9 (as above) as the *G2*-specific primer. The amplified products were cloned in pGEM T-Easy vector (Promega) and sequenced.

Sequencing and analysis of sequence data: Plasmid subclones containing cDNA and genomic sequences generated in cloning or by PCR were fully sequenced on both strands using a Sequenase kit (Amersham, Buckinghamshire, UK) or by an automated sequencing facility (ABI). Sequence contigs were assembled using GeneJockey II software (BioSoft; Cambridge, UK).

Isolation of RNA and gel blot analysis: RNA was isolated, electrophoresed on 1.5% formaldehyde-agarose gels, blotted onto Nytran membranes (Schleicher and Schuell, Keene, NH) over 48 hr and hybridized as reported in Langdale *et al.* (1988b). The *Ppc1*, *Ppdk1*, *Mdh1*, *Mod1*, *RbcS*, *rbcL*, and *ubiquitin* cDNA clones have been described previously (Langdale and Kidner 1994; Hall *et al.* 1998).

Transmission electron microscopy: Tissue samples were cut under fixative (3% formaldehyde, 3% glutaraldehyde, 0.0025 M phosphate buffer, pH 7.2), vacuum infiltrated, and then left for 2 hr at room temperature. Samples were washed three times for 20 min in 0.0025 M phosphate buffer pH 7.2 and then incubated in 2% OsO_4 for 1 hr. Following three further washes in 0.0025 M phosphate buffer pH 7.2, the samples were dehydrated through an acetone series. Samples were then gradually infiltrated with 25% TAAB resin:acetone (TAAB Laboratory Equipment, Reading, UK) followed by 50% TAAB: acetone for 8 hr and 100% TAAB overnight. The resin was polymerized at 60° for 24 hr. Ultrathin sections (100 nm) were cut using a glass knife on a Sorvall MT5000 microtome. Sections were mounted on Butvar B98 slots (Agar Aids, Essex, UK) and stained using a 2168 Ultrostainer Carlsberg System (Leica) in Ultrostain1 (Leica) for 2 hr and Ultrostain2 (Leica) for 10 min according to the manufacturer's instructions. Sec-

tions were examined using a Jeol JEM-2000 EX transmission electron microscope and photographed using AGFA (Leverkusen, Germany) Scientia EM film 23 D 56.

RESULTS

Structure of the *G2* locus in the B73 inbred line: To isolate a wild-type *G2* locus, a maize genomic library prepared from the inbred line B73 was screened using a previously isolated cDNA (Hall *et al.* 1998). A 5.2-kb contig was sequenced and shown to contain the entire *G2* coding region, intervening introns, 710 bases upstream of the start of transcription and 11 bases downstream of the end of exon 5 (GenBank accession no. AF298118). There are 411 untranslated nucleotides in the 5′ region of exon 1 and 395 untranslated nucleotides in the 3′ region of exon 5. A putative open reading frame (ORF) of 57 amino acids was identified in the 5′ untranslated region. Upstream open reading frames have been identified in a number of genes and are thought to regulate translation of the downstream gene (Damiani and Wessler 1993). Whether this small ORF plays a similar role in the regulation of *G2* remains to be determined.

Genotypic characterization of mutant *g2* alleles: Four mutations in the *G2* gene have been characterized (summarized in Figure 1). Three of the alleles, *g2-bsd1-m1*, *g2-bsd1-s1*, and *g2-pg14*, represent insertions of an *Spm* transposable element into the *G2* gene. The fourth mutation, *g2-R*, is not transposon induced and instead has a number of small alterations in the gene sequence.

In *g2-bsd1-s1*, a 3-kb defective *Spm* element is inserted in the 3′ to 5′ orientation in intron 2, 144 bp after the start of the intron. This insertion site corresponds to position 2415 of the *G2* genomic sequence. Comparison with the published *Spm* sequence (Pereira *et al.* 1985) revealed that 5265 nucleotides corresponding to positions 1370–6634 of *Spm* are deleted in the inserted element. In *g2-bsd1-m1*, the site and orientation of *Spm* insertion is the same as in *g2-bsd1-s1*; however, the element is autonomous. The fact that the *Spm* insertion site is identical in the two alleles supports the suggestion (Hall *et al.* 1998) that *g2-bsd1-s1* is a deletion derivative of *g2-bsd1-m1*.

The *g2-pg14* allele was previously reported to result from the insertion of an autonomous *Spm* element into the *G2* gene (Peterson 1953). PCR of genomic DNA revealed that the element is inserted in the 5′ to 3′ orientation at position −76 of the *G2* locus, 3 bp upstream of the putative TATA box. Additional changes alter three amino acids in exon 1 (see Figure 1 legend), but it is unlikely that these alterations perturb G2 function because revertant sectors are observed in *g2-pg14* plants. Thus, when the element excises, the gene is functional.

The *g2-R* allele was first identified in an inbreeding experiment and the nature of the mutation was unknown (Jenkins 1927). Initially, therefore, experiments were carried out to determine whether *G2* transcripts accumulate in *g2-R* mutant plants. RNA gel blot analysis demonstrated that *G2* transcripts accumulate at a lower level in *g2-R* mutant plants than in wild type and furthermore that the transcript is ~300 bp shorter (1.9 kb) than the wild-type transcript (2.2 kb; Figure 2). PCR amplification from both *g2-R* genomic DNA and cDNA prepared from *g2-R* leaf tissue indicated that this size difference is due to differences in polyadenylation. Polyadenylation can occur at position 1965 (mutant form), 2067 (undetected on Northern blots), and 2183 (wild-type form) of the wild-type cDNA sequence.

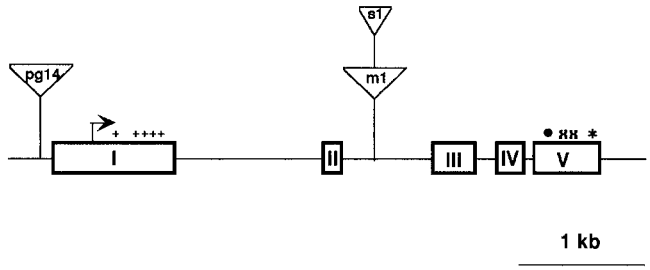

Figure 1.—Genomic structure of *g2* alleles. Intron positions within the *G2* genomic locus were established by comparing genomic and cDNA sequences. The locus comprises five exons of 969, 141, 345, 171, and 564 bp, separated by four introns of 1199, 760, 214, and 108 bp. The 5′ end of exon 1 is predicted on the basis of sequence analysis of the longest *G2* cDNA clone identified (Hall *et al.* 1998). Outlined boxes represent exons in the wild-type gene and are numbered accordingly. The start of transcription is marked by an arrow and the position of the stop codon by a dot.The wild-type (B73) polyadenylation signal is marked by an asterisk. *Spm* element insertion sites in *g2-bsd1-m1*, *g2-bsd1-s1*, and *g2-pg14* are represented by triangles. In *g2- pg14*, three amino acid alterations are also seen in exon 1: a substitution of T for C at position 433 results in the replacement of an arginine residue with a cysteine. A 3-bp insertion between 492 and 493 adds an extra valine residue, and an inversion of the bases at positions 533 and 534 substitutes a cysteine residue with a serine. The extra polyadenylation sites used in *g2-R* are shown by x. Exon 1 is 24 bp shorter than predicted and the position of insertions and deletions are indicated by plus signs. A 9-bp deletion corresponding to positions 475–483 (inclusive) deletes three glycine residues, whereas two extra glycine residues are encoded by a 6-bp insertion between positions 786 and 787. Deletions of nucleotides 799–801 and 883–885 remove two alanines and a further deletion between positions 835 and 849 (inclusive) removes four threonine residues and a glutamic acid residue. Further alterations include a substitution of T to C at position 603 that represents a neutral substitution in an alanine codon, a C to G at position 710 that changes alanine to glycine, a C to G at position 717 that changes aspartic acid to glutamic acid, and a C to T at position 805 that substitutes serine for alanine.

Phenotypic characterization of *g2* mutants: To determine the phenotypic consequence of each *g2* mutation, mutant plants were characterized with respect to whole plant phenotype, *G2* transcript levels, levels of transcripts encoding photosynthetic enzymes, and chloro-

plast ultrastructure. All four alleles were introgressed four times into the inbred line B73 prior to analysis.

Whole plant phenotype: The macroscopic effects of each *g2* mutation are similar but subtle differences were observed between the four mutations. *g2-bsd1-m1* mutant plants were identified by their pale green leaf blades that exhibited dark green revertant sectors. Revertant tissue represented 0–50% of each leaf. In contrast, the leaf blades of *g2-bsd1-s1* mutant plants were a uniform pale green. The leaf sheaths of *g2-bsd1-m1* and *g2-bsd1-s1* plants were white but, in the case of *g2-bsd1-m1* plants, pale green revertant sectors were also observed. *g2-bsd1-s1* plants were distinguished very early in development because mutant coleoptiles were paler than wild type. *g2-pg14* mutants exhibited leaf blades that were only slightly paler green than those of wild-type plants and leaf sheaths that were very pale yellow. In the *g2-pg14* genetic stock used for this study, reversion events were infrequent and, as such, mutants exhibited an essentially stable phenotype. However, if mutant plants were outcrossed to another inbred line, *Spm* excision events were activated and revertant sectors were observed. Thus, a functional G2 protein is produced following *Spm* excision from the promoter. *g2-R* mutant plants were a yellow-green color and leaf sheaths were white. Like *g2-bsd1-s1* individuals, *g2-R* mutant plants were identified early in development by their pale coleoptiles. None of the mutations examined appeared to affect germination processes. In both the light and the dark, germination rates appeared normal, and during the seedling stages of development mutant plants developed at the same rate as their wild-type siblings.

C_4 photosynthetic leaf blades: G2 transcripts have previously been shown to accumulate predominantly in C_4 leaf blade tissue of wild-type plants (Hall *et al.* 1998). To further investigate transcript levels in wild-type and mutant leaf blade tissue, Northern blot analysis of RNA isolated from the base and tip of third leaf blades was carried out (Figure 2A). In wild-type leaves, a 2.2-kb transcript was detected at roughly equivalent levels throughout the blade. In leaves of each of the *g2* mutants, *G2* transcripts accumulated at a much lower level than that seen in wild-type plants. No *G2* transcript could be detected in mutant sectors of *g2-bsd1-m1* leaf blades. In *g2-bsd1-s1* and *g2-R* mutants, transcript size was different from that seen in wild-type leaves. In *g2-bsd1-s1* mutants, the hybridizing transcript was ~4.2 kb, while in *g2-R*, the transcript was 1.9 kb. As described previously, the 4.2-kb transcript in *g2-bsd1-s1* also hybridizes to *Spm*

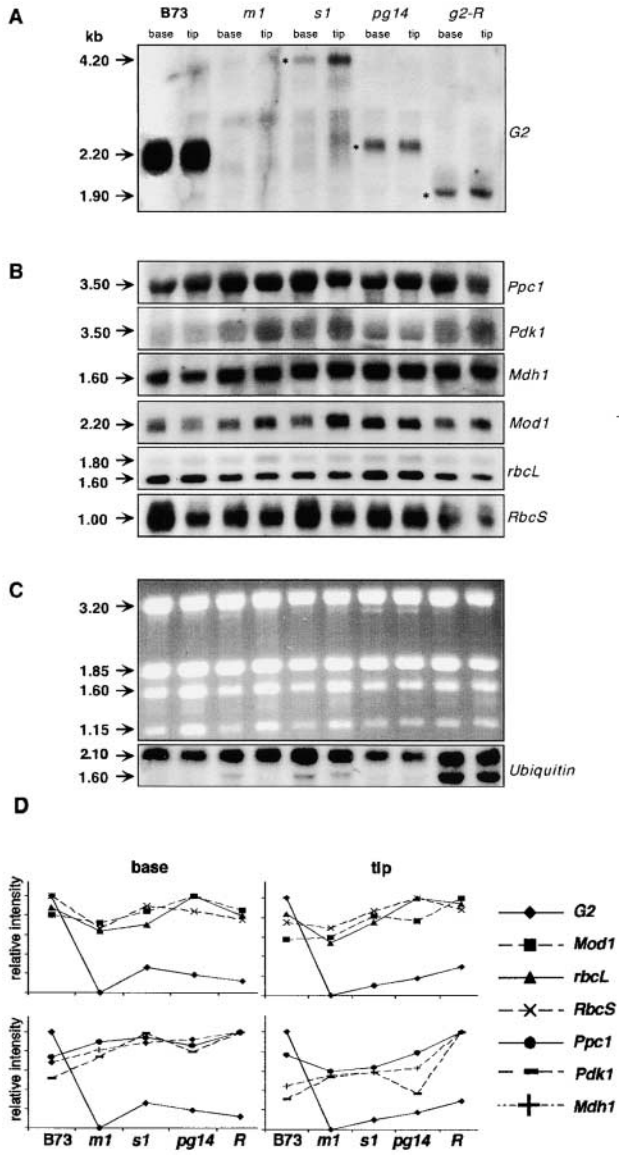

Figure 2.—Transcript accumulation in wild-type and mutant third leaf blades. (A) RNA gel blot analysis of *G2* transcripts. Leaf blades were divided into base and tip sections. *G2* transcripts in mutant samples are indicated by asterisks. Transcript size is shown at the left. Because the autoradiograph had to be exposed for a long time to reveal the presence of transcripts in mutant samples, a negative shadowing effect can be seen where the 3.2- and 1.9-kb ribosomal RNAs transferred to the filter. (B) RNA gel blot analysis of C_4 transcripts. The same filter used in A showing hybridization of mesophyll-specific (*Ppc1*, *PpdK1*, and *Mdh1*) and bundle sheath-specific (*RbcS*, *rbcL*, and *Mod1*) transcripts. Transcript size is shown at the left. (C) Control of RNA quality and quantity. (Top) Ethidium bromide staining of the gel used for blotting. Ribosomal RNA sizes are indicated. (Bottom) The filter used in A hybridized to ubiquitin. Two ubiquitin transcripts are observed corresponding to seven and five ubiquitin repeats (Christensen and Quail 1989). (D) Densitometric analysis of blots shown in A–C. Hybridization signals were normalized to the intensity of ethidium bromide staining measured using a Biorad Fluor-S Multimager. Because density of signal on the autoradiographs may not represent hybridization in a linear fashion, hybridization signals were then subsequently expressed relative to the maximum intensity measured for a particular probe in a particular tissue. In this way, accumulation profiles could be compared although accurate measurements of mRNA levels could not be obtained. Results obtained for the experiment shown are representative of others carried out with independent tissue samples.

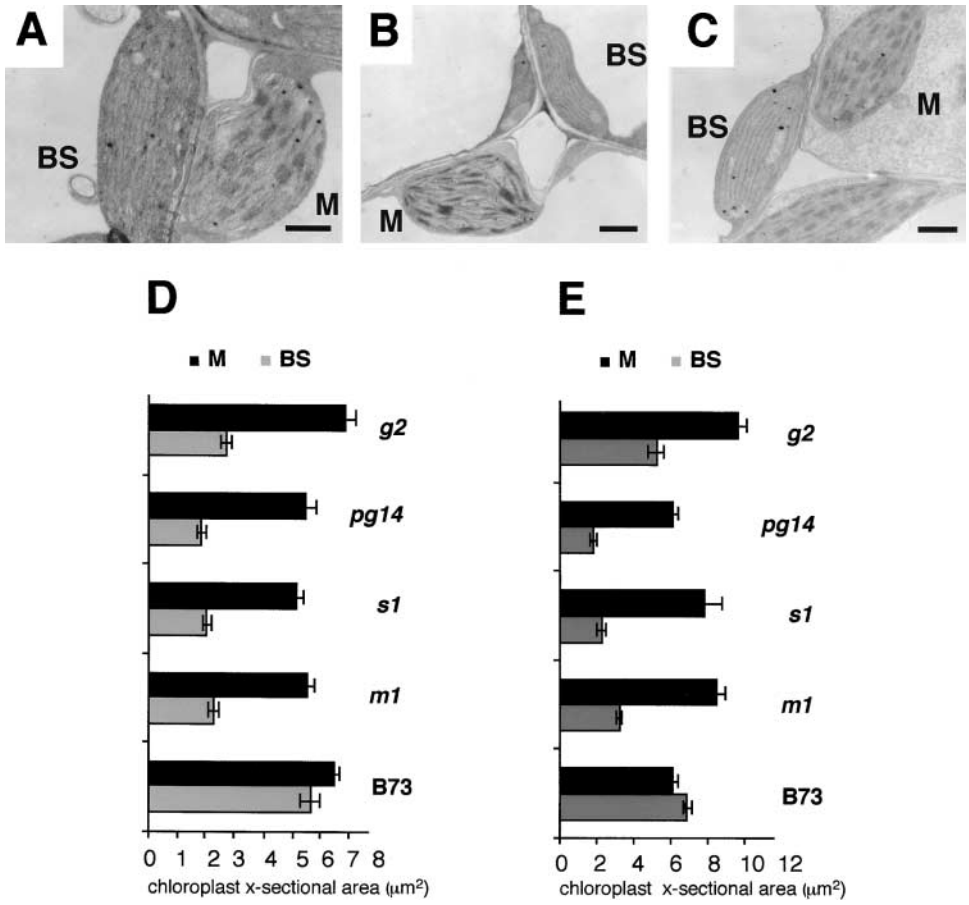

FIGURE 3.—Chloroplast ultrastructure in wild-type and mutant third leaf blades. (A–C) Electron micrographs showing bundle sheath (BS) and mesophyll (M) chloroplasts at the base of wild-type and mutant leaves. (A) Wild type (B73). (B) *g2-pg14*. (C) *g2-R*. (D) Mean cross-sectional area of chloroplasts at the leaf base with standard error. (E) Mean cross-sectional area of chloroplasts at the leaf tip with standard error. Bar, 1 μm.

and thus represents a *G2/Spm* chimera (HALL *et al.* 1998). The 1.9-kb transcript in *g2-R* samples may encode a functional protein because the entire coding region is present; however, the amino acid alterations observed in exon 1 may alter functional potential.

To determine whether *G2* transcript levels correlate with levels of transcripts encoding photosynthetic enzymes, Northern blot analysis was carried out to assess the levels of bundle sheath cell-specific (*rbcL*, *RbcS*, and *Mod1*, which encodes ME) and mesophyll cell-specific (*Ppc1*, *PdK1*, and *Mdh1*) transcripts. It was previously reported that bundle sheath cell-specific transcripts are either absent or present at only very low levels in *g2-bsd1-m1* mutant leaf blades (LANGDALE and KIDNER 1994). In this study, where *g2* mutants have been analyzed after introgression into the inbred line B73, perturbations to bundle sheath cell-specific transcript accumulation patterns were less apparent (Figure 2B). When accumulation profiles of *G2* and transcripts encoding photosynthetic enzymes were compared (Figure 2D), no obvious correlation was seen between the two. Notably, however, in *g2-bsd1-m1* leaves where *G2* transcripts could not be detected, both bundle sheath- and mesophyll-specific transcripts accumulated. Thus, in C_4 leaf blades, G2 is not required for the direct transcriptional regulation of genes encoding carbon fixation enzymes. Photosynthetic enzyme proteins also accumulated to normal levels in all mutant tissues examined (data not shown), further indicating that G2 is not required for post-transcriptional processing of C_4 mRNAs.

Transmission electron microscopy (TEM) was used to investigate whether perturbations to chloroplast ultrastructure could be related to *G2* transcript levels in mutant leaves. The dimorphic chloroplasts characteristic of maize were clearly visible in wild-type third leaf blades used in this study (KIRCHANSKI 1975; Figure 3A). Mesophyll chloroplasts contain stacked thylakoid membranes, lack starch grains, and are arranged randomly within the cell. Bundle sheath chloroplasts are more elliptical in shape than those of the mesophyll cells and are arranged centrifugally within the cell, in contact with the cell wall that is adjacent to the mesophyll. Bundle sheath chloroplasts have agranal thylakoids and accumulate starch grains within the stroma. In each mutant, the *g2* mutation conditioned defective chloroplast morphology specifically in the bundle sheath cells (Figure 3, B–E). Bundle sheath chloroplasts at the leaf base were much smaller than their wild-type counterparts and exhibited only rudimentary lamellae. Mesophyll chloroplasts appeared structurally normal and did not differ in size from wild type. The phenotype was most severe in *g2-pg14* mutants (Figure 3B) and least severe in *g2-R* mutant plants (Figure 3C). Although *G2* transcript levels cannot be directly correlated with per-

turbations to chloroplast structure, the results presented in Figures 2 and 3 demonstrate that reduced levels of *G2* transcripts in third leaf blades consistently impact on bundle sheath cell chloroplast development.

C_3 etiolated leaves: Etiolated maize leaves display a C_3 type of photosynthetic differentiation in that RuBPCase accumulates in both bundle sheath and mesophyll cells (Sheen and Bogorad 1986; Langdale *et al.* 1988b). Previous studies of *g2-bsd1-m1* mutant plants showed that differentiation was disrupted in both cell types of etiolated leaves in that RuBPCase did not accumulate (Langdale and Kidner 1994). To assess further the role of G2 in the development of this C_3 state, the *G2* expression profile was examined in etiolated and light-shifted leaves of all four *g2* mutants (Figure 4A). *G2* transcripts accumulate in both dark- and light-grown tissue. In etiolated leaves of all four mutants, transcript levels were noticeably reduced relative to wild-type levels. In light-shifted leaves, *G2* transcripts also accumulated to lower levels in mutants than in wild type, although the reduction was not as severe as that observed in etiolated tissue. The detection of *G2* transcripts in etiolated and light-shifted *g2-bsd1-m1* leaves appears to contradict results obtained with third leaf blades. However, as we were unable to score etiolated and light-shifted tissues for the presence of revertant sectors, these samples most likely represent a mosaic of mutant and revertant tissue. In *g2-bsd1-s1* mutant light-shifted leaves, a 2.1-kb transcript was observed in addition to the 4.2-kb transcript. This second transcript has been observed previously in this mutant but it is not known whether it is translated into a functional protein (Hall *et al.* 1998). The predominant transcript detected in *g2-R* tissue was the 1.9-kb form; however, very low levels of the wild-type 2.2-kb form were also seen. The 2.2-kb transcript was not detected in any other *g2-R* tissues.

Although etiolated leaves are nonphotosynthetic, transcripts encoding most of the C_4 photosynthetic enzymes eventually accumulate in wild-type plants. To assess whether levels of these transcripts correlate with *G2* transcript levels in mutant plants, transcript accumulation patterns were examined in both etiolated and light-shifted tissue. In both wild-type and mutant plants, both bundle sheath- and mesophyll-specific transcripts accumulate to higher levels in light-shifted tissue than in etiolated leaves (Figure 4B). In etiolated leaves of *g2-bsd1-s1* plants, as in *g2-bsd1-m1* third leaf blades, transcripts encoding photosynthetic enzymes accumulated in the absence of *G2* transcripts. Thus, no strict correla-

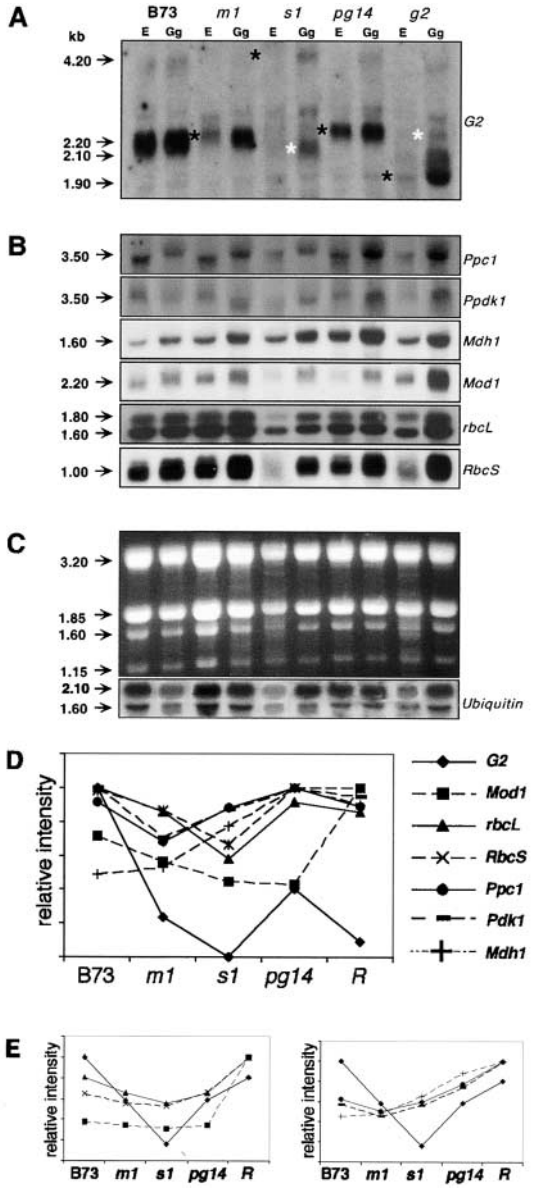

Figure 4.—Transcript accumulation in wild-type and mutant etiolated leaves. (A) RNA gel blot analysis of *G2* transcripts in etiolated (E) and light-shifted (Gg) wild-type and mutant leaves. *G2* transcripts in mutant samples are indicated by asterisks. The alternative 2.1-kb *G2* transcript observed in light-shifted *g2-bsd1-s1* leaves and the 2.2-kb transcript observed in *g2-R* tissue are indicated by white asterisks. Transcript size is shown at the left. Because the autoradiograph had to be exposed for a long time to reveal the presence of transcripts in mutant samples, a negative shadowing effect can be seen where the 3.2- and 1.9-kb ribosomal RNAs transferred to the filter. (B) RNA gel blot analysis of C_4 transcripts. The same filter was used in A showing hybridization to mesophyll-specific (*Ppc1*, *PpdK1*, and *Mdh1*) and bundle sheath-specific (*RbcS*, *rbcL*, and *Mod1*) transcripts. Transcript size is shown at the left. (C) Control of RNA quality and quantity. (Top) Ethidium bromide staining of the gel used for blotting. Ribosomal RNA sizes are indicated. (Bottom) The filter used in A hybridized to ubiquitin. (D) Densitometric analysis of etiolated samples shown in blots A–C. Samples were analyzed as for Figure 2D. Results obtained for the experiment shown are representative of others carried out with independent tissue samples. (E) Densitometric analysis of light-shifted samples shown in A–C. Samples were analyzed as for Figure 2D. Probes are as indicated in Figure 4D. Results obtained for the experiment shown are representative of others carried out with independent tissue samples.

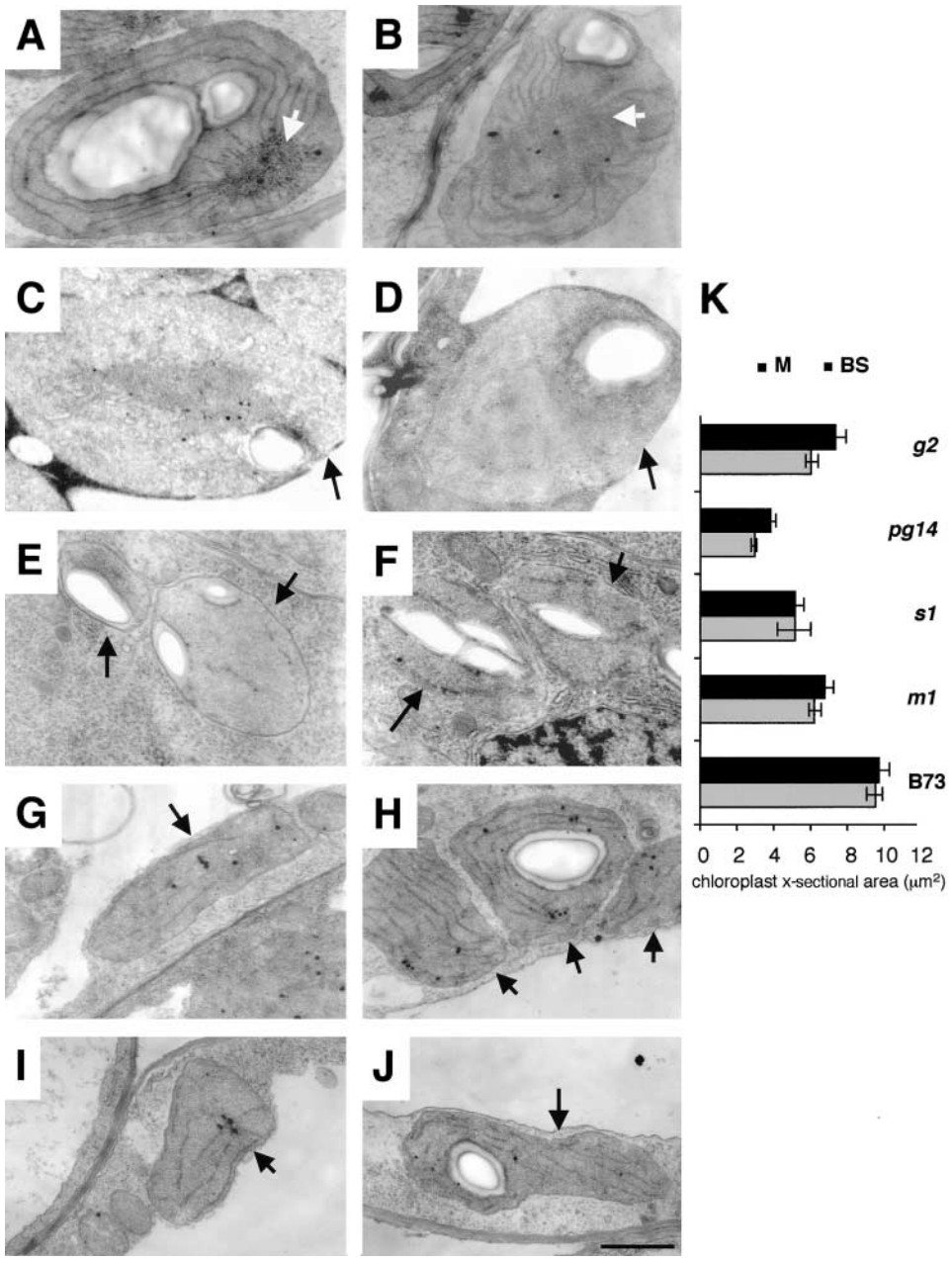

FIGURE 5.—Chloroplast ultrastructure in wild-type and mutant etiolated leaves. (A–J) Electron micrographs showing bundle sheath (A, C, E, G, and I) and mesophyll (B, D, F, H, and J) plastids in etiolated leaves. Solid arrows point to etioplasts; open arrows point to the prolamellar body. (A and B) Wild-type leaves. (C and D) *g2-bsd1-m1* leaves. (E and F) *g2-bsd1-s1* leaves. (G and H) *g2-pg14* leaves. (I and J) *g2-R* leaves. (K) Mean cross-sectional area of etioplasts in wild-type and mutant leaves with standard error.

tion existed between the accumulation profiles of *G2* and transcripts encoding the photosynthetic enzymes (Figure 4D). However, RuBPCase protein does not accumulate in etiolated mutant plants (LANGDALE and KIDNER 1994; data not shown) and a loose correlation can be seen between accumulation profiles of *G2*, *RbcS*, and *rbcL* transcripts. This suggests that G2 has more influence on RuBPCase accumulation in this C_3 type tissue than in C_4 leaf blades. In light-shifted tissue, *G2* transcript levels were consistently lower in mutant plants than in wild type. However, levels of transcripts encoding photosynthetic enzymes were roughly equivalent to wild type if not higher in mutant plants (Figure 4, B and E). Therefore, with the caveat that complete absence of *G2* transcripts was not observed in this tissue in any mutant, the increase in transcript levels following exposure to light appears to be independent of G2 function.

In contrast to the non-cell-specific effect of *g2-bsd1-m1* on RuBPCase accumulation in etiolated leaves, previous investigations suggested that the *g2-bsd1-m1* mutation specifically affects bundle sheath cells in terms of etioplast morphology (LANGDALE and KIDNER 1994). To address further the question of cell specificity in dark-grown leaves, etioplast morphology in mutant plants was examined by TEM (Figure 5, A–K). Wild-type etioplasts were morphologically identical in bundle sheath and mesophyll cells (Figure 5, A and B). Prolamellar bodies were distinguished in etioplasts of both cell types and further internal membranes radiating from this structure were clearly visible. Etioplasts in *g2* mutant plants

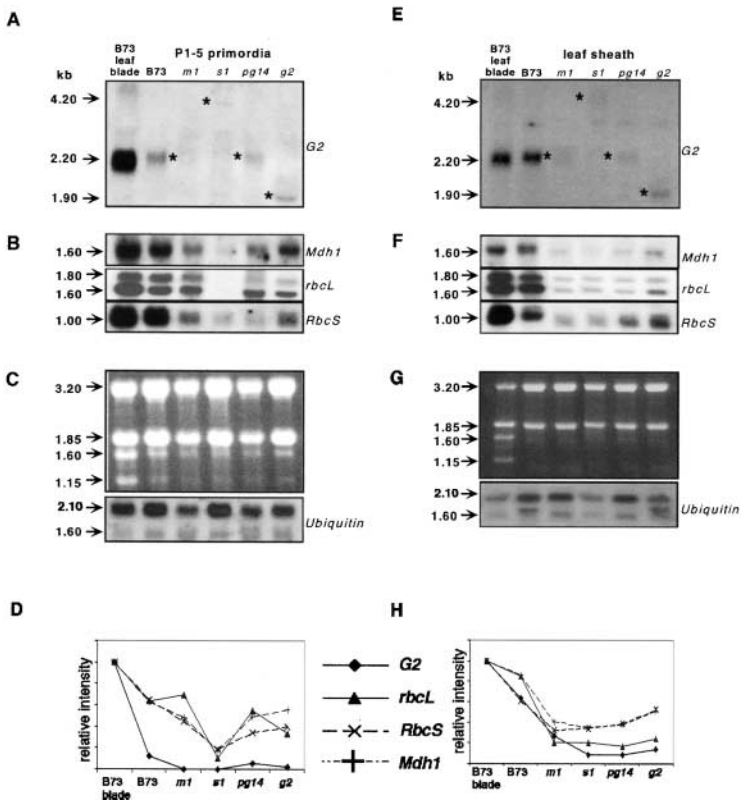

FIGURE 6.—Transcript accumulation in immature leaf tissue. (A) RNA gel blot analysis of *G2* transcripts in wild-type and mutant P1-5 primordia. *G2* transcripts in mutant samples are indicated by asterisks. Transcript size is shown at the left. (B) RNA gel blot analysis of C_4 transcripts in wild-type and mutant P1-5 primordia. The same filter used in A showing hybridization to mesophyll-specific (*Mdh1*) and bundle sheath-specific (*RbcS*, *rbcL*) transcripts. Transcript size is shown at the left. (C) Control of RNA quality and quantity. (Top) Ethidium bromide staining of the gel used for blotting. Ribosomal RNA sizes are indicated. (Bottom) The filter used in A hybridized to ubiquitin. (D) Densitometric analysis of blots shown in A–C. Samples were analyzed as for Figure 2D. Results obtained for the experiment shown are representative of others carried out with independent tissue samples. (E) RNA gel blot analysis of *G2* transcripts in wild-type and mutant leaf sheaths. *G2* transcripts in mutant samples are indicated by asterisks. Transcript size is shown at the left. (F) RNA gel blot analysis of C_4 transcripts in wild-type and mutant leaf sheaths. The same filter used in D showing hybridization to *Mdh1*, *RbcS*, and *rbcL* transcripts. Transcript size is shown at the left. (G) Control of RNA quality and quantity. (Top) Ethidium bromide staining of the gel used for blotting. Ribosomal RNA sizes are indicated. (Bottom) The filter used in E hybridized to ubiquitin. (H) Densitometric analysis of blots shown in E–G. Samples were analyzed as for Figure 2D. Results obtained for the experiment shown are representative of others carried out with independent tissue samples. Bar, 1 μm.

did not exhibit prolamellar bodies and only small quantities of internal membrane that did not originate from an obvious center were observed (Figure 5, C–J). Mesophyll and bundle sheath cell etioplasts could not be distinguished except by cell position. In these respects, the mutant plastids were similar to proplastids, albeit larger, and it is possible that they represent less developed etioplasts than the wild-type examples. Previously, prolamellar bodies were observed in both mesophyll and bundle sheath etioplasts, but bundle sheath etioplasts were found to be smaller than wild type (LANGDALE and KIDNER 1994). The tissue examined in the previous study was harvested at a later stage in development than tissue examined here and it is therefore possible that the *g2* mutations initially delay etioplast development in both cell types but that this delay becomes more pronounced in bundle sheath cells later in development. Alternatively, the difference may reflect the consequence of perturbed G2 function in different genetic backgrounds. Notably, these results demonstrate that in etiolated leaves, as in third leaf blades, decreased *G2* transcript levels consistently lead to perturbed plastid development.

Immature leaf tissue: Whereas etiolated leaves are nonphotosynthetic due to lack of exposure to light, leaf primordia and young leaf sheath tissue are nonphotosynthetic as a consequence of developmental immaturity. These two tissues differ, however, in that leaf primordia will eventually develop into C_4 photosynthetic tissue whereas leaf sheaths will eventually form intermediate C_4/C_3 structures. In mutant leaf primordia and leaf sheaths, *G2* transcript levels were reduced to varying degrees in each *g2* mutant as compared to wild type (Figure 6, A and B). In the pre-C_4 leaf primordia, *G2* transcripts were barely detectable in *g2-bsd1-s1* and *g2-bsd1-m1* mutants (Figure 6A). In the pre-C_4/C_3 sheath tissue, *G2* transcript levels were very low and were roughly equivalent in all four mutants (Figure 6E). With the exception of *g2-bsd1-m1*, *G2* transcript levels in *g2* mutants were reduced in third leaf sheaths to a similar extent as that seen in third leaf blades. In *g2-bsd1-m1*, the decrease in transcript levels was less severe in leaf sheaths than in leaf blades. Once again, however, this may reflect the presence of revertant tissue in the sample.

To examine the effect of reduced *G2* transcript levels in immature tissue on the accumulation of transcripts encoding photosynthetic enzymes, Northern blots were carried out. In wild-type P1-5 leaf primordia only *Mdh1*, *rbcL*, and *RbcS* transcripts accumulate. *Mdh1* accumulates in mesophyll progenitor cells and *rbcL* and *RbcS* accumulate in bundle sheath progenitor cells (LANGDALE *et al.* 1988b). In immature leaf sheath tissue, the same three transcripts predominate but *RbcS* and *rbcL* accumulate in both cell types while *Mdh1* accumulates only in mesophyll cells (LANGDALE *et al.* 1988a). In mutant P1-5 *g2-bsd1-m1* leaf primordia, all three transcripts accumulated in the absence of detectable *G2* transcript (Figure 6B) and no obvious correlation was observed between accumulation profiles (Figure 6D). In *g2-bsd1-s1*

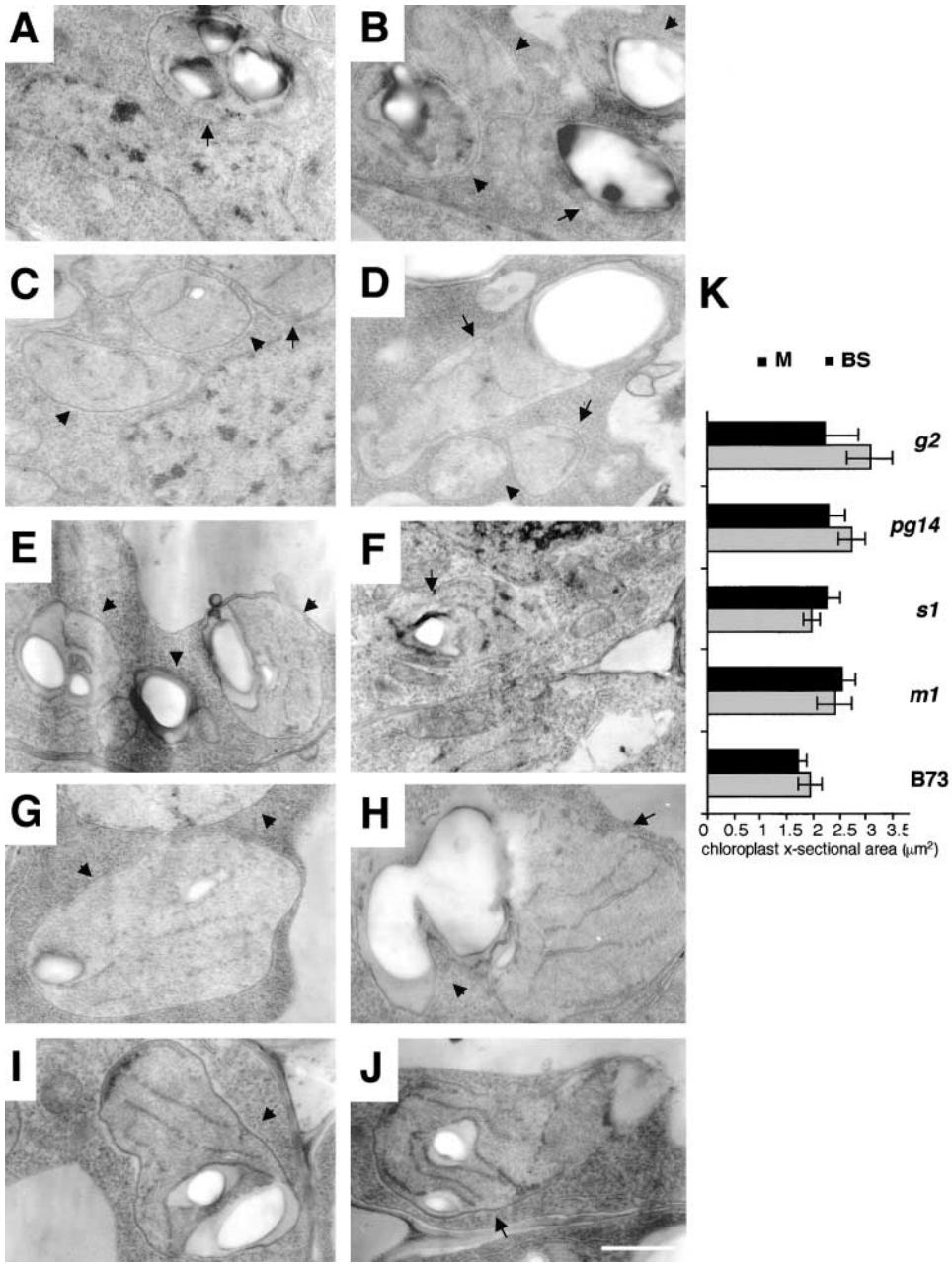

FIGURE 7.—Chloroplast ultrastructure in immature leaf tissue. (A–J) Electron micrographs showing bundle sheath (A, C, E, G, and I) and mesophyll (B, D, F, H, and J) plastids in P5 leaf primordia. Solid arrows point to proplastids. (A and B) Wild-type leaves. (C and D) *g2-bsd1-m1* leaves. (E and F) *g2-bsd1-s1* leaves. (G and H) *g2-pg14* leaves. (I and J) *g2-R* leaves. (K) Mean cross-sectional area of proplastids in wild-type and mutant leaves with standard error. Bar, 1 μm.

mutants, transcript levels were particularly low, possibly reflecting a general delay in the onset of photosynthetic development following germination. In mutant leaf sheath tissue, levels of *rbcL*, *RbcS*, and *Mdh1* were all lower than in wild type (Figure 6F) and accumulation profiles reflected those of *G2* transcripts (Figure 6H). However, because the 4.2-kb transcript in *g2-bsd1-s1* represents a chimera of *G2* and *Spm* sequences, this correlation may not be strict with respect to G2 function.

To determine whether chloroplast ultrastructure is perturbed in immature mutant leaf tissue, TEM was carried out on P5 leaf primordia. Bundle sheath and mesophyll plastids in wild-type P5 leaves resembled the proplastids found in meristematic cells, in that they were small, roughly spherical, and exhibited only minimal thylakoid membrane structures (Figure 7, A and B). It was not possible to distinguish between mesophyll and bundle sheath plastids at this stage and identification was made by cell position. In all *g2* mutants, plastids in both cell types were indistinguishable from wild type and resembled proplastids in that they were small, spherical, and contained only minimal quantities of internal membrane (Figure 7, C–K). These results suggest that any effect of the *G2* gene product on chloroplast ultrastructure is not visible until after plastochron 5.

DISCUSSION

The development of photosynthetic tissues in maize is influenced by light-induced signals that are interpreted differently depending on cell position relative to a vein (LANGDALE and NELSON 1991). In this way, cells differ-

entiate as C_4 bundle sheath (light induced, adjacent to a vein), C_4 mesophyll (light induced, adjacent to a bundle sheath), or C_3 mesophyll (light induced, greater than two cells from a vein or etiolated). Any model to account for how G2 functions in this process must consider the phenotype of *g2* mutants. In C_4 photosynthesizing tissue such as third leaf blades and greening leaves, consistent perturbations to bundle sheath cell chloroplast structure are observed when *G2* transcript levels are reduced (Figure 3). In contrast, bundle sheath cell-specific transcripts encoding photosynthetic enzymes can accumulate and all aspects of mesophyll cell development can occur in the absence of G2 (Figures 2 and 3). G2 is therefore unlikely to regulate photosynthetic gene expression or mesophyll chloroplast development directly. Thus, G2 has a specific role in C_4 photosynthesizing tissue, namely, to facilitate normal bundle sheath cell chloroplast development.

In C_3 tissue such as immature leaf sheaths and etiolated tissue, both chloroplast structure and RuBPCase accumulation patterns are perturbed in the absence of G2 (Figures 4, 5, and 6). As G2 plays no direct role in the accumulation of photosynthetic enzymes in C_4 leaf blade tissue, the simplest explanation for the observed phenotype in C_3 tissue is that the absence of RuBPCase is a secondary consequence of perturbed plastid development. If this is the case, the role of G2 in both C_3 mesophyll and C_4 bundle sheath cells is to facilitate normal plastid development. Therefore, the different effects on photosynthetic enzyme accumulation patterns in mutant tissue most likely reflect the relative importance of plastid competence within any particular tissue. For example, in C_4 leaf blade tissue, signals such as light, which directly promote photosynthetic gene expression, presumably exert more influence on accumulation patterns than plastid signals. Thus, in C_4 tissue, enzyme accumulation patterns are relatively normal despite perturbed plastid development whereas, in C_3 tissue, disruption of plastid development disrupts enzyme accumulation patterns.

A feature of *g2* mutant individuals observed both in this and previous investigations is the phenotypic recovery in older tissues leading to a partial restoration of wild-type characteristics. In this study, mutant bundle sheath cell chloroplasts at the tip of mutant leaf blades exhibited a less severe defect than that seen at the base of the leaf. This difference in chloroplast structure was not correlated with a difference in *G2* transcript levels (Figure 2A). Although it is possible that transcript levels may not reflect levels of the active *G2* gene product, these data suggest that phenotypic recovery is mediated by something other than G2. We have recently identified a gene in maize (*ZmGlk1*) that has extensive sequence similarity to *G2* (Rossini *et al.* 2001). In *g2* mutant plants, *ZmGlk1* transcripts are present at normal levels (J. A. Langdale, unpublished data). Because low levels of *ZmGlk1* transcripts accumulate in C_4 bundle sheath cells of wild-type leaves (Rossini *et al.* 2001), it is therefore possible that ZmGLK1 mediates the eventual recovery of bundle sheath cell chloroplasts in *g2* mutant leaf blades.

On the basis of the *g2* mutant phenotypes reported here and the analysis of *G2* and *ZmGlk1* expression patterns (Rossini *et al.* 2001), we propose a model to explain photosynthetic cell-type differentiation in maize. In C_3 tissues, it is proposed that G2 acts to facilitate normal chloroplast development. In etiolated leaves, the absence of light leads to etioplast development whereas the presence of light in C_3 mesophyll cells facilitates the proplastid-to-chloroplast conversion. It is proposed that G2 has an indirect (positive) effect on the accumulation of RuBPCase in these cell types. At this stage of development and in these tissues, *ZmGlk1* transcripts are barely detectable (Rossini *et al.* 2001). In C_4 tissues, however, light promotes the accumulation of *ZmGlk1* transcripts, primarily in C_4 mesophyll cells and *G2* transcripts accumulate preferentially in C_4 bundle sheath cells (Hall *et al.* 1998; Rossini *et al.* 2001). We therefore propose that in C_4 tissues, ZmGLK1 acts primarily to facilitate C_4 mesophyll chloroplast development whereas G2 facilitates chloroplast development in C_4 bundle sheath cells.

We thank Gulsen Akgun and Cledwyn Merriman for technical support and John Baker for photography. We are grateful to all members of the lab for constructive discussions throughout the course of this work, particularly Laura Rossini and Dave Martin for critical reading of the manuscript. We thank Debbie Alexander for help with statistics. This work was supported by grants from the Biotechnological and Biological Sciences Research Council (BBSRC) and the Gatsby Charitable Foundation to J.A.L. L.C. was the recipient of a BBSRC research studentship.

LITERATURE CITED

Chen, J., and S. L. Dellaporta, 1994 Urea-based plant DNA miniprep, pp. 526–528 in *The Maize Handbook*, edited by M. Freeling and V. Walbot. Springer Verlag, New York.

Christensen, A. H., and P. H. Quail, 1989 Sequence analysis and transcriptional regulation by heat shock of polyubiquitin transcripts from maize. Plant Mol. Biol. **12:** 619–633.

Damiani, R. D., and S. R. Wessler, 1993 An upstream open reading frame represses expression of *Lc*, a member of the *R/B* family of maize transposable activators. Proc. Natl. Acad. Sci. USA **90:** 8244–8248.

Edwards, G. E., and D. A. Walker, 1983 *C_3, C_4: Mechanisms and Cellular and Environmental Regulation of Photosynthesis.* Blackwell Scientific, Oxford.

Hall, L. N., and J. A. Langdale, 1996 Molecular genetics of cellular differentiation in leaves. Tansley review No. 88. New Phytol. **132:** 533–553.

Hall, L. N., L. Rossini, L. Cribb and J. A. Langdale, 1998 GOLDEN2: a novel transcriptional regulator of cellular differentiation in the maize leaf. Plant Cell **10:** 925–936.

Jenkins, M. T., 1927 A second gene producing golden plant color in maize. Am. Nat. **60:** 484–488.

Kirchanski, S. J., 1975 The ultrastructural development of the dimorphic plastids of *Zea mays* L. Am. J. Bot. **62:** 695–705.

Langdale, J. A., and C. A. Kidner, 1994 *bundle sheath defective*, a mutation that disrupts cellular differentiation in maize leaves. Development **120:** 673–681.

Langdale, J. A., and T. Nelson, 1991 Spatial regulation of photosynthetic development in C_4 plants. Trends Genet. **7:** 191–196.

Langdale, J. A., B. A. Rothermel and T. Nelson, 1988a Cellular patterns of photosynthetic gene expression in developing maize leaves. Genes Dev. **2:** 106–115.

Langdale, J. A., I. Zelitch, E. Miller and T. Nelson, 1988b Cell position and light influence C_4 versus C_3 patterns of photosynthetic gene expression in maize. EMBO J. **7:** 3643–3651.

Nelson, T., and J. A. Langdale, 1992 Developmental genetics of C_4 photosynthesis. Annu. Rev. Plant Physiol. Plant Mol. Biol. **43:** 25–47.

Pereira, A., Z. Schwarz-Sommer, A. Gierl, I. Bertram, P. A. Peterson *et al.*, 1985 Genetic and molecular analysis of the enhancer transposable element system of *Zea mays.* EMBO J. **4:** 17–23.

Peterson, P. A., 1953 A mutable pale green locus in maize. Genetics **38:** 682.

Rossini, L., L. Cribb, D. J. Martin and J. A. Langdale, 2001 The maize *Golden2* gene defines a novel class of transcriptional regulators in plants. Plant Cell **13:** 1231–1244.

Sheen, J.-Y., and L. Bogorad, 1986 Expression of the ribulose-1,5-bisphosphate carboxylase large subunit gene and three small subunit genes in two cell types of maize leaves. EMBO J. **5:** 3417–3422.

Communicating editor: K. J. Newton